

Change of optical properties of inorganic perovskite nanocrystals of $\text{CsPbCl}_x\text{Br}_{3-x}$, alloyed with Yb^{3+} ions, when carrying out an anion exchange reaction

© D.A. Tatarinov¹, A.V. Sokolova¹, D.V. Danilov², A.P. Litvin¹

¹ Information Optical Technology Center, Quantum Nanostructures Optics Laboratory, ITMO University, 197101 St. Petersburg, Russia

² Interdisciplinary Resource Center for Nanotechnologies, St. Petersburg State University, 199034 St. Petersburg, Russia

e-mail: litvin@itmo.ru

Received June 13, 2022

Revised June 13, 2022

Accepted June 17, 2022

Alloying of perovskites nanocrystals by lanthanoids makes it possible to produce materials that luminesce effectively in both visible and near infrared spectra. In the present work, the influence of the width of the forbidden zone on the optical properties of the inorganic perovskites nanocrystals $\text{CsPbCl}_x\text{Br}_{3-x}$ alloyed by ions Yb^{3+} is investigated. For changing the chemical composition of nanocrystals, an anionic exchange method is used by adding bromide dodecyltrimethylammonium. As a result of the gradual substitution of chlorine ions with bromine ions, the forbidden area of nanocrystals is narrowed, resulting in a change in the spectral position of the optical transitions, the quantum output of photoluminescence in the near and infrared spectral ranges and the attenuation of photoluminescence. When the width of the forbidden area reaches 2.54 eV, the total quantum output of photoluminescence reaches 72%.

Keywords: perovskite nanocrystals, alloying, ytterbium, photoluminescence, anionic exchange.

DOI: 10.21883/EOS.2022.08.54778.2772-22

1. Introduction

Lead metal halides inorganic nanocrystals (NC) with perovskite structure and chemical formula CsPbX_3 ($X = \text{Cl}, \text{Br}, \text{I}$) are currently actively investigated material that has a wide range of different applications, including optoelectronics, nonlinear optics, photovoltaics, catalysis, sensory and quantum information technologies [1–4]. In this context, great attention is paid by the scientific community to various methods of modifying perovskite NC in order to change their optical properties [5] and improve stability under different conditions [6,7]. Alloying is one of the widely used approaches, the application of which allows to increase the quantum output of photoluminescence (QO PL) [8–10] and to promote the enhancement of nonlinear optical responses [11,12].

In addition to the above mentioned properties, alloying with lanthanides, in particular ytterbium ions (Yb^{3+}), results in an additional band in the near infrared (IR) region of the spectrum. Due to this, it is possible to obtain new nanomaterials with unique properties, which is interesting for the creation of effective and stable sources of near infrared radiation, luminescent labels, as well as increasing the efficiency of solar batteries and solar concentrators [13–15]. The large number of potential applications indicates the multifunctionality of perovskite NC, which significantly increases the relevance of their research.

In NC CsPbX_3 : Yb^{3+} position of the PL band in the infrared spectrum range is associated with the energy transition of Yb^{3+} ions, and therefore it is fixed for each particular lanthanide. At the same time, the position of PL maximum in the visible part of the spectrum, belonging to the matrix (NC CsPbX_3), can be configured by post-synthetic NC processing by an anionic exchange reaction [16,17]. The structure of the perovskite has a sufficiently high mobility of anions, which allows it to be replaced partially or completely with other halogens. Therefore, the PL band can be accurately rebuilt across the visible spectral range while maintaining high quality optical responses. An anionic exchange also allows precise regulation of the width of the forbidden area (E_g) and, therefore, to investigate its influence on the emission properties of various alloying impurities in the perovskite matrix, such as manganese [16], ytterbium [17], erbium [18], cerium [19] etc. In addition, the control of the width of the forbidden area makes it possible to accurately select the optimal composition of the anionic subarray of NC to achieve the maximum QO PL depending on the required tasks.

Different precursors [20–22] can be used to change the anion composition and thus the width of the forbidden area of the perovskite matrix. When fully inorganic halogen compounds are used, QO PL bands of alloying impurities can be significantly reduced in the near infrared spectrum region. Another disadvantage of this approach is the low stability of the NC obtained at high levels of the precursor halogen. To

minimize these disadvantages, it is important to react in the inert atmosphere and to use organohalogenides as anions by virtue of their passivating properties. Examples of such compounds are tetra-octylammonium bromide (TOAB) and dodecyltrimethylammonium bromide (DDAB) [23]. With the right selection of suitable chemical agents and anionic exchange conditions, it is possible to obtain alloyed NC perovskite not only with the required optical properties, but also with high stability.

In the present work the dependence of optical properties of reference and Yb^{3+} ions alloyed NC perovskites $\text{CsPbCl}_x\text{Br}_{3-x}$ from the width of the forbidden area was investigated. The halogen ratio in nanocrystals was varied by partial anionic exchange with the addition of DDAB. Dependencies of change of optical properties of NC perovskites when replacing ions Cl^- with Br^- ions as part of the perovskite matrix have been identified.

2. Materials and research techniques

Reference NC CsPbCl_3 were obtained by injecting caesium oleate into a chlorine and lead precursor solution at a temperature of 180°C [24]. The perovskite ($\text{Yb}^{3+}:\text{CsPbCl}_3$) NC alloyed with Yb^{3+} ions were obtained by injecting the caesium oleate into a solution of chlorine, lead and terbium precursors at 260°C temperature, according to the report, described in the work [18]. Upon completion of the NC synthesis process, the process of removing the reaction mixture and washing the NC from excess ligands was carried out.

The shape and size of the received NC $\text{Yb}^{3+}:\text{CsPbCl}_3$ have been investigated with the help of translucent electron microscopy (TEM), the resulting images are presented in Fig. 1. Nanocrystals are nanoparticles with a shape close to cubic, while the average face size is 12 ± 3 nm (Fig. 2).

The optical properties of NC were studied in a toluene solution. In the reaction of exchange of Cl^- ions with Br^- ions, a DDAB solution with a concentration of $C_{\text{DDAB}} = 0.4$ M in toluene was used in the perovskite matrix. The anion exchange was conducted in an inert atmosphere, after which the ditch with the solution was tightly sealed. At the same time, the chemical

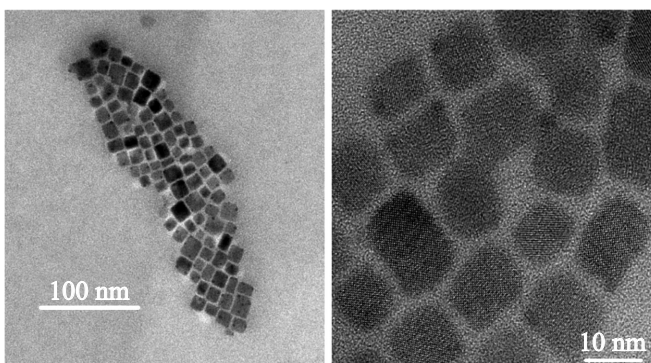


Figure 1. TEM images of NC $\text{Yb}^{3+}:\text{CsPbCl}_3$.

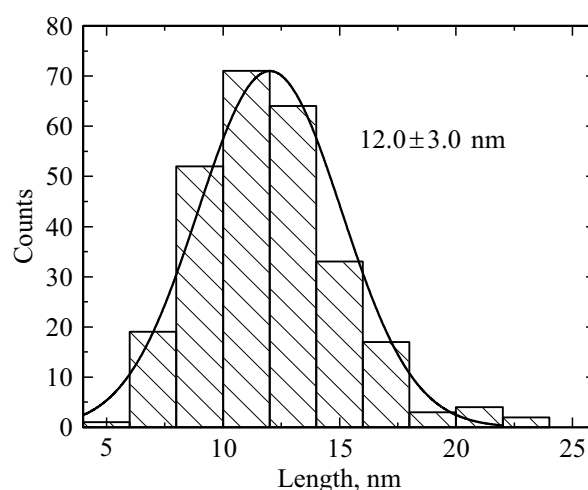


Figure 2. Analysis of the mean face length of quasi-cubic NC $\text{Yb}^{3+}:\text{CsPbCl}_3$.

composition of NC and, as a consequence, the width of the forbidden area changed smoothly. For each sample, absorption and PL spectra (visible and near IR ranges) and PL attenuation curves (near IR range) were recorded.

Absorption spectra were measured using a Shimadzu UV-3600 spectrophotometer. The PL spectra are derived using an experimental complex for detecting PL in the visible and near IR ranges described in the works [25,26]. The 375 nm laser was used as the source of the exciting radiation. To study the attenuation kinetics of PL, an avalanche InGaAs/InP photodiode (Micro Photon Devices) was used, PL was excited by a pulse laser with a wavelength of 351 nm and a pulse repetition frequency of 100 Hz. TEM images were obtained by Zeiss Libra 200FE microscope at an accelerating voltage of 200 kV.

3. Results and discussion

The absorption and PL spectra for a number of reference $\text{CsPbCl}_x\text{Br}_{3-x}$ NC and those alloyed by Yb^{3+} $\text{HK Yb}^{3+}:\text{CsPbCl}_3$ ions are given in Fig. 3. It is obvious that when the degree of ion substitution of Cl^- with Br^- ions decreases the width of the forbidden area and, as a result, shifts the PL band to the long-wave area of the visible part of the spectrum. At the same time, for both types of NC there is a gradual increase in the intensity of PL until the value of ~ 2.5 eV is reached, after which the intensity of PL in the visible spectral range dramatically decreases, and the spectra exhibit a clear asymmetry.

Based on absorption spectroscopy data, the width of the forbidden area for each sample was calculated using the Tautz graphs, as shown in the inset to Fig. 3, a. The dependence of the obtained values of E_g on the amount of DDAB added for the tested samples is shown in Fig. 4. Note that the dependencies obtained for both reference and

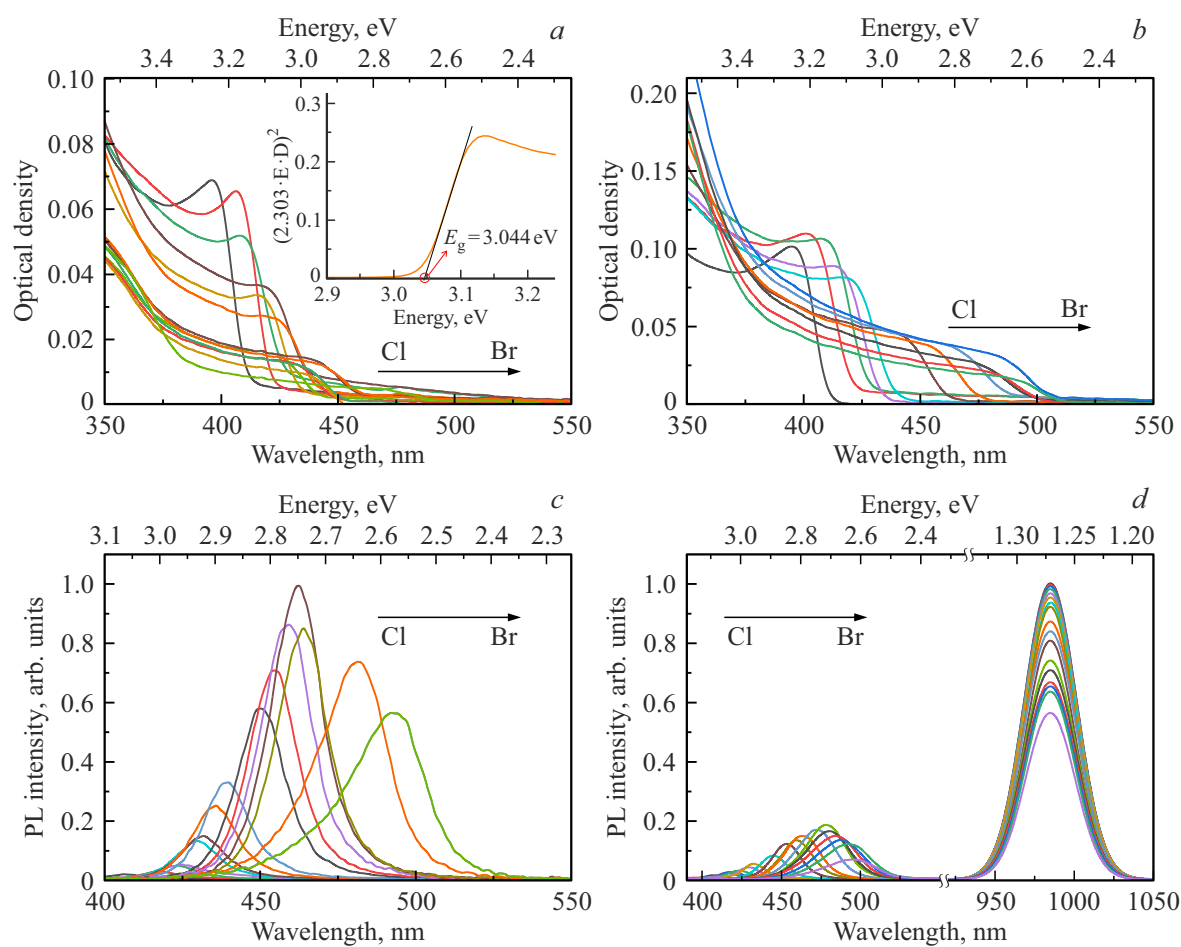


Figure 3. Absorption spectra (*a, b*) and PL (*c, d*) for NC CsPbCl_xBr_{3-x} (*a, c*) and Yb³⁺:CsPbCl_xBr_{3-x} (*b, d*) with different degree of replacement of Cl ions with Br ions.

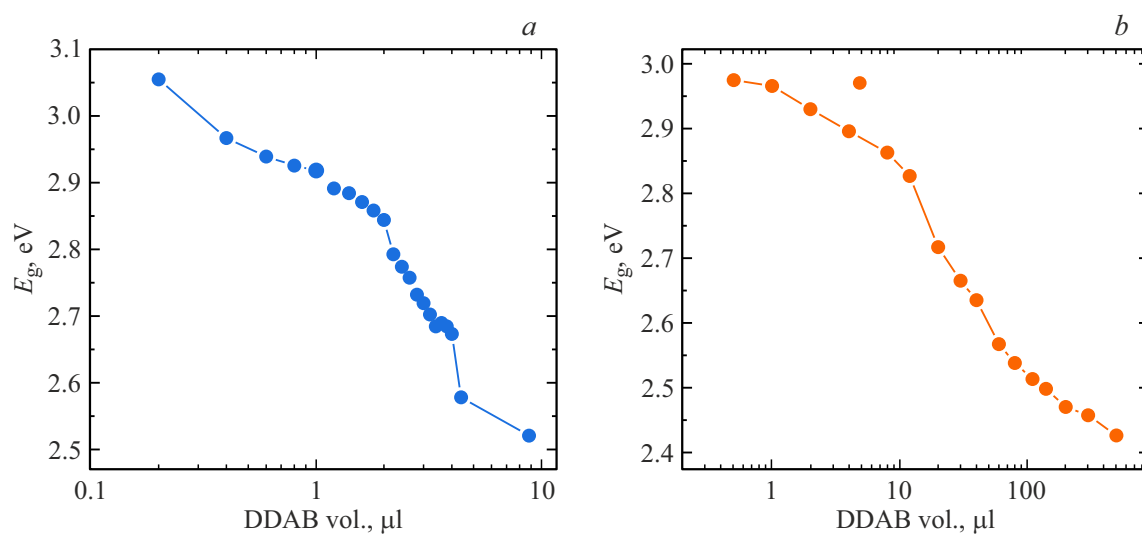


Figure 4. The dependencies of the forbidden area width for (*a*) NC CsPbCl_xBr_{3-x} and (*b*) NC Yb³⁺:CsPbCl_xBr_{3-x} on the volume of added DDAB ($C_{DDAB} = 0.4$ M).

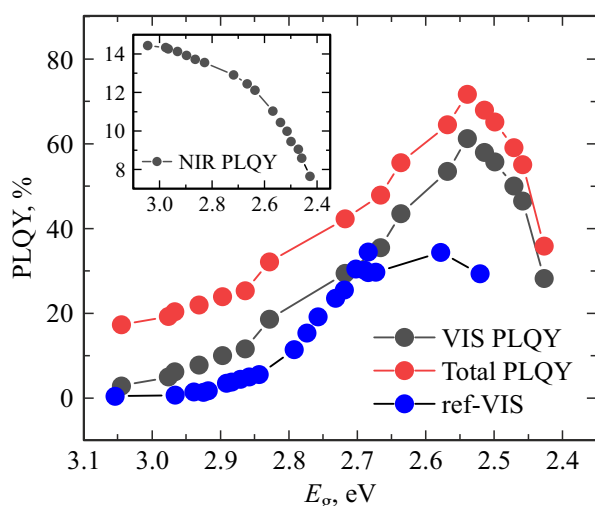


Figure 5. The dependence of QO PL on the width of the forbidden area of NC. Blue curve — QO-PL within the visible spectral range for reference samples of NC $\text{CsPbCl}_x\text{Br}_{3-x}$. The black and red curves — respectively QO PL within the visible spectral range and the total QO PL for NC $\text{Yb}^{3+}:\text{CsPbCl}_x\text{Br}_{3-x}$ samples. Inset — dependency of QO PL on the width of the forbidden NC area in the near IR range for NC samples $\text{Yb}^{3+}:\text{CsPbCl}_x\text{Br}_{3-x}$.

alloyed NC are qualitatively matched, which indicates that the alloying of NC does not affect the process of replacing their anion subarray. In both cases, complete replacement of anions cannot be achieved.

For reference and alloyed NC values of QO PL in visible and near IR ranges were calculated with known values of QO PL (rhodamine 6Zh and quantum PbS points respectively). QO PL dependencies for reference and doped NC $\text{CsPbCl}_x\text{Br}_{3-x}$ are shown in Fig. 5. With the addition of DDAB solution, QO PL of reference samples increases, which is caused by both a decrease of E_g (a decrease in the number of deep traps) [27], and the passivation of their surface by DDAB molecules. The resulting QO PL dependencies in the visible range are qualitatively the same for alloyed and reference NC, but the increase in QO PL when reducing the width of the forbidden area is greater for NC $\text{Yb}^{3+}:\text{CsPbCl}_x\text{Br}_{3-x}$. This may be due to a gradual reduction in the efficiency of transferring photoexcitations from the perovskite matrix to Yb^{3+} impurity ions, which is an additional relaxation channel for excited electron states in the matrix. This assumption is supported by a gradual decrease in the intensity of Yb^{3+} PL ions in the near IR range with a decrease in the width of the forbidden area (inset in Fig. 5). This process is sharper at a width of the forbidden area of less than 2.7 eV and is accompanied by a significant increase in QO PL in the visible spectral range. At the width of the forbidden area ~ 2.54 eV reaches the maximum value of the total QO PL, which is 72%. In large DDAB additives, there is a decrease in PL intensity for both reference and alloyed NC, which may be

caused by an excess of passivating agents in the solution, resulting in partial destruction of NC and impairment of their optical properties. This correlates with the broadening and asymmetry of the corresponding PL spectra as shown in Fig. 3.

For NC $\text{Yb}^{3+}:\text{CsPbCl}_x\text{Br}_{3-x}$ with different width of the forbidden area, curves of PL Yb^{3+} ions in the near IR spectrum area were obtained and photoluminescence lifetimes were calculated. The PL attenuation curves have been described by a monoexponential function with the time constant of a few milliseconds, which quite well corresponds with the literary data [28–30]. Examples of PL attenuation curves for NC with different halogen ratios Cl/Br are shown in Fig. 6, *a*. The resulting dependence of PL attenuation times on the width of the forbidden NC alloyed area is shown in Fig. 6, *b*. There is a gradual reduction in the attenuation time of PL, which goes to saturation after reaching the width of the forbidden area less than ~ 2.7 eV. Similar observations published in the work [28] were explained by the change in the crystal field surrounding Yb^{3+} ions in NC $\text{Yb}^{3+}:\text{CsPbCl}_x\text{Br}_{3-x}$. For large DDAB additives, there is a sharp reduction in the PL attenuation time, which is correlated with the results obtained for QO PL and can be caused by the degradation of NC.

4. Conclusion

Reference perovskite NC CsPbCl_3 and ytterbium ion-alloyed NC $\text{Yb}^{3+}:\text{CsPbCl}_3$ were obtained by hot injection. The addition of DDAB to NC solutions has allowed the NC anionic subarray to be gradually changed, with a consequent reduction in the width of their forbidden area. Thus, lines of NC samples of $\text{CsPbCl}_x\text{Br}_{3-x}$ and $\text{Yb}^{3+}:\text{CsPbCl}_x\text{Br}_{3-x}$ with different chemical compositions were obtained. The dependences of optical properties of reference and alloyed ions Yb^{3+} NC from the width of the forbidden area have been investigated. It has been shown that a change in the width of the forbidden area leads to a change in the QO PL in the visible and near IR spectral ranges, as well as a change in the attenuation time of PL of the Yb^{3+} ions. The total QO PL of alloyed specimens reaches 72% at the width of the forbidden area 2.54 eV. The results obtained in the work can be used for producing new nanomaterials with effective PL in a wide spectrum range for use in optoelectronics, solar energy and biomedicine.

Acknowledgments

The authors express their gratitude to the employees of the Interdisciplinary Resource Center in the direction of „Nanotechnologies“ of the Science Park of Saint Petersburg State University for the help in obtaining TEM images of samples.

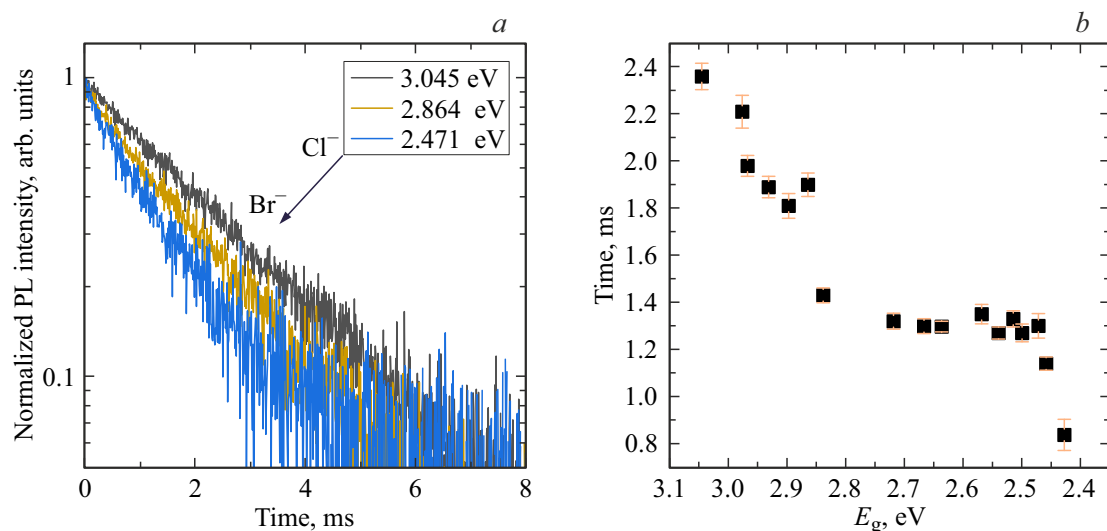


Figure 6. (a) PL attenuation curves for multiple samples of NC $\text{Yb}^{3+}:\text{CsPbCl}_x\text{Br}_{3-x}$ solutions with different forbidden area width, (b) PL attenuation time dependence on the forbidden area width NC.

Funding

The study was carried out with the support of PSF within the framework of scientific project No 21-73-10131, as well as a grant from NIRMA FT MF of ITMO University.

Conflict of interest

The authors declare that they have no conflict of interest.

References

- [1] Z. Cao, F. Hu, C. Zhang, S. Zhu, M. Xiao, X. Wang. *Adv. Photonics*, **2** (5), 8–10 (2020). DOI: 10.1117/1.AP.2.5.054001
- [2] X. Mei, D. Jia, J. Chen, S. Zheng, X. Zhang. *Nano Today*, **43** 101449 (2022). DOI: 10.1016/j.nantod.2022.101449
- [3] W. Shen, J. Chen, J. Wu, X. Li, H. Zeng. *ACS Photonics*, **8** (1), 113–124 (2021). DOI: 10.1021/acsp Photonics.0c01501
- [4] M. Liu, G. K. Grandhi, S. Matta, K. Mokurla, A. Litvin, S. Russo, P. Vivo. *Adv. Photonics Res.*, **2** (3), 2000118 (2021). DOI: 10.1002/adpr.202000118
- [5] Y. Chen, Y. Liu, M. Hong. *Nanoscale*, **12** (23), 12228–12248 (2020). DOI: 10.1039/d0nr02922j
- [6] S. Zou, Y. Liu, J. Li, C. Liu, R. Feng, F. Jiang, Y. Li, J. Song, H. Zeng, M. Hong et al. *J. Am. Chem. Soc.*, **139** (33), 11443–11450 (2017). DOI: 10.1021/jacs.7b04000
- [7] C. Bi, S. Wang, Q. Li, S.V. Kershaw, J. Tian, A.L. Rogach. *J. Phys. Chem. Lett.*, **10** (5), 943–952 (2019). DOI: 10.1021/ACS.JPCLETT.9B00290/SUPPL_FILE/JZ9B00290_SL001.PDF
- [8] J.S. Yao, J. Ge, B.N. Han, K.H. Wang, H. Bin Yao, H.L. Yu, J.H. Li, B.S. Zhu, J.Z. Song, C. Chen et al. *J. Am. Chem. Soc.*, **140** (10), 3626–3634 (2018). DOI: 10.1021/jacs.7b11955
- [9] Z.J. Yong, S.Q. Guo, J.P. Ma, J.Y. Zhang, Z.Y. Li, Y.M. Chen, B. Bin Zhang, Y. Zhou, J. Shu, J.L. Gu et al. *J. Am. Chem. Soc.*, **140** (31), 9942–9951 (2018). DOI: 10.1021/jacs.8b04763
- [10] M. Lu, X. Zhang, Y. Zhang, J. Guo, X. Shen, W.W. Yu, A.L. Rogach. *Advanced Materials*, 1804691, 1–6 (2018). DOI: 10.1002/adma.201804691
- [11] R. Ketavath, N.K. Katturi, S.G. Ghugal, H.K. Kolli, T. Swetha, V.R. Soma, B. Murali. *J. Phys. Chem. Lett.*, **10** (18), 5577–5584 (2019). DOI: 10.1021/acs.jpclett.9b02244
- [12] I.D. Skurlov, W. Yin, A.O. Ismagilov, A.N. Tcypkin, H. Hua, H. Wang, X. Zhang, A.P. Litvin, W. Zheng. *Nanomaterials*, **12** (1), 1–16 (2022). DOI: 10.3390/nano12010151
- [13] W.J. Mir, T. Sheikh, H. Arfin, Z. Xia, A. Nag. *NPG Asia Mater.*, **12** (1), 1–9 (2020). DOI: 10.1038/s41427-019-0192-0
- [14] S. Kachhap, S. Singh, A.K. Singh, S.K. Singh. *J. Mater. Chem. C*, **10** (10), 3647–3676 (2022). DOI: 10.1039/D1TC05506B
- [15] B. Su, G. Zhou, J. Huang, E. Song, A. Nag, Z. Xia. *Laser Photon. Rev.*, **15** (1), 2000334 (2021). DOI: 10.1002/LPOR.202000334
- [16] W. Liu, Q. Lin, H. Li, K. Wu, I. Robel, J. M. Pietryga, V.I. Klimov. *J. Am. Chem. Soc.*, **138** (45), 14954–14961 (2016). DOI: 10.1021/jacs.6b08085
- [17] T.J. Milstein, K.T. Kluherz, D.M. Kroupa, C.S. Erickson, J.J. De Yoreo, D.R. Gamelin. *Nano Lett.*, **19** (3), 1931–1937 (2019). DOI: 10.1021/acs.nanolett.8b05104
- [18] X.X. Zhang, Y. Zhang, X.X. Zhang, W. Yin, Y. Wang, H. Wang, M. Lu, Z. Li, Z. Gu, W.W. Yu. *J. Mater. Chem. C*, **6** (37), 10101–10105 (2018). DOI: 10.1039/c8tc03957g
- [19] D. Zhou, D. Liu, G. Pan, X. Chen, D. Li, W. Xu, X. Bai, H. Song. *Adv. Mater.*, **29** (42), 1704149 (2017). DOI: 10.1002/adma.201704149
- [20] G. Nedelcu, L. Protesescu, S. Yakunin, M.I. Bodnarchuk, M.J. Grotevent, M.V. Kovalenko. *Nano Lett.*, **15** (8), 5635–5640 (2015). DOI: 10.1021/acs.nanolett.5b02404
- [21] Q.A. Akkerman, V. D’Innocenzo, S. Accornero, A. Scarpellini, A. Petrozza, M. Prato, L. Manna. *J. Am. Chem. Soc.*, **137** (32), 10276–10281 (2015). DOI: 10.1021/jacs.5b05602
- [22] T. J. Milstein, D. M. Kroupa, D. R. Gamelin. *Nano Lett.*, **18** (6), 3792–3799 (2018). DOI: 10.1021/acs.nanolett.8b01066

- [23] S. Yang, C. Bi, J. Tian. *J. Phys. Chem. C*, **125** (34), 18810–18816 (2021). DOI: 10.1021/acs.jpcc.1c04896
- [24] L. Protesescu, S. Yakunin, M.I. Bodnarchuk, F. Krieg, R. Caputo, C.H. Hendon, R.X. Yang, A. Walsh, M.V. Kovalenko. *Nano Lett.*, **15** (6), 3692–3696 (2015). DOI: 10.1021/nl5048779
- [25] P.S. Parfenov, A.P. Litvin, E.V. Ushakova, A.V. Fedorov, A. V. Baranov, K. Berwick. *Rev. Sci. Instrum.*, **84** (11), 116104 (2013). DOI: 10.1063/1.4829717
- [26] I.D. Skurlov, D.A. Onishchuk, P.S. Parfenov, A.P. Litvin. *Opt. Spectrosc.*, **125** (5), 756–759 (2018). DOI: 10.1134/S0030400X18110279
- [27] A. Dey, J. Ye, A. De, E. Debroye, S.K. Ha, E. Bladt, A.S. Kshirsagar, Z. Wang, J. Yin, Y. Wang et al. *ACS Nano*, (2021). DOI: 10.1021/acsnano.0c08903
- [28] H. Huang, R. Li, S. Jin, Z. Li, P. Huang, J. Hong, S. Du, W. Zheng, X. Chen, D. Chen. *ACS Appl. Mater. Interfaces*, **13** (29), 34561–34571 (2021). DOI: 10.1021/acsnano.1c09421
- [29] M. Stefanski, M. Ptak, A. Sieradzki, W. Strek. *Chem. Eng. J.*, **408** (September 2020), (2021). DOI: 10.1016/j.cej.2020.127347
- [30] J.Y. D. Roh, M.D. Smith, M.J. Crane, D. Biner, T.J. Milstein, K.W. Krämer, D.R. Gamelin. *Phys. Rev. Mater.*, **4** (10), 1–11 (2020). DOI: 10.1103/PhysRevMaterials.4.105405